

A Proposal for a Multi-Function Materials Facility for the Spallation Neutron Source

Colin G Windsor and Roger N Sinclair

Materials Physics and Metallurgy Division, AERE, Harwell , OX11 0RA.

Summary. A neutron beam instrument is proposed which will allow the simultaneous study of the microstructural, crystalline phase, internal stress, defect, local order, texture, diffusional and vibrational properties of materials. The penetration of neutrons permits all these properties to be studied in a bulk specimen *in situ* during a heat treatment or chemical reaction as a function of time. The possibility of using narrow incident and scattered neutron beams allows the simultaneous monitoring of these properties as a function of position across the sample. Only by using the polychromatic neutron beam from a pulsed source, can all these properties be studied at the same time and at the same point on the specimen. The proposed instrument is designed for installation on the Spallation Neutron Source recently commissioned at the Rutherford Appleton Laboratory. Its performance is evaluated for a series of key experiments in applied science and shown to permit a complete neutron examination of the sample within minutes.

1. Introduction

Conventional neutron instruments are restricted to just one of the many neutron techniques which can be applied to a sample. Their counters record only a tiny fraction of the precious neutrons scattered by the sample. This proposal demonstrates that the restriction can be overcome by using a variety of detector banks together with the wide incident wavelength band given by a pulsed source. A series of techniques can be matched together in a single *multi-facility* with little compromise on the performance of any one mode. The present design considers an instrument optimised for the resolution and intensities required when applying neutron techniques to materials science.

The ability of neutron beams to penetrate several centimetres of most materials makes them uniquely useful in materials science(1). Whole components may be studied with little surface preparation or sensitivity to surface effects. The same penetrating ability allows easy containment of the component in a furnace, stress cell or reaction vessel. This makes possible the *in situ* study of irreversible processes such as the ageing of steels, the creep to fracture of a tensile specimen, or the setting of a cement. The several techniques of neutron beam science are often performed consecutively on different specimens and on different instruments. The proposed instrument allows the principal neutron beam techniques to be applied to the same specimen at the same time. A second feature of this instrument is its use of a thin *pencil* incident neutron beam to scan the properties of the sample as a function of position across its surface. For example the microvoids, defect structure, minority phases and stress could be measured across a fracture specimen with resolution of a few millimetres. Its 90° angle counters allow properties, such as residual stress and texture within a weld, to be measured as a function of three-dimensional position within the volume of the sample.

The thinking behind this instrument is illustrated by recent developments in electron microscopy. When a feature of interest is found by transmission microscopy, a battery of techniques— electron diffraction, X-ray analysis, Auger analysis and electron energy loss spectroscopy can all be applied to the same area of the specimen. Neutron scattering offers an even wider range of complementary techniques.

The wide range of usable neutron scattering angles and incident wavelengths enables a series of diffractometers to be tailored to different scientific objectives. These are characterised by different, if overlapping, ranges in the scattering vector $Q=4\pi\sin(\phi/2)/\lambda$ depending on the scattering angle ϕ and wavelength λ . The size range monitored is given roughly by $L\approx 2\pi/Q$ so that the different Q ranges are analogous to the different magnifications of a microscope. The accessible Q values span a range of 10^4 from 0.004 to 40 \AA^{-1} implying a size range from many hundreds to a fraction of an Angstrom. The range of resolution ΔQ feasible in neutron diffraction is equally wide. It needs to be matched to the required precision in the size of the object under study. Even at the same value of Q there is a need for both high resolution and low resolution measurements. For example around $Q = 2 \text{\AA}^{-1}$, corresponding to typical interatomic spacings, high resolution diffraction defines the sharp d-spacings of crystallites. At the same time local order in a defect structure or multi-component liquid reveals short range structure which requires only low resolution. The need is for the widest possible range of Q vectors to be covered at a range of resolutions ΔQ . Such is the objective of this instrument.

A unique feature of neutron scattering is that it embraces both structural studies through diffraction, and dynamic studies through the Doppler shifts caused by atomic motions. Diffusion in the sample gives quasi-elastic broadening with a width proportional to the rate of diffusion, while vibrations give inelastic modes at the energy transfer $\hbar\omega$ corresponding to the vibrational frequency ω . Most inelastic experiments have lower counting rates than is usual in diffraction. This instrument uses only configurations of relaxed resolution that can be operated together with diffraction in time and spatially resolved experiments.

2. The principal fields in materials science covered by neutron scattering.

A recent review considered the contributions of neutron beam techniques to applied materials science (2). The principal areas are given in table 1 together with complementary techniques.

(i) Microstructure.

The use of Small Angle Neutron Scattering (SANS) to probe microstructure in the size range 30 to 1000 Å⁻¹ has proved one of the most powerful fields of materials science (3). Although its upper size range is covered by electron microscopy, SANS offers an easy and quantitative route to a defect diameter distribution function and volume fraction measurement. As conventionally practised, with a Q value range from of order 0.006 to 0.3 Å⁻¹, SANS has the important limitation that the nature of the defects being observed is not known except when evident from other information. However many defects studied by SANS will also give an observable diffraction pattern. For example, a 200 Å diameter particle gives a diffraction peak at a 2Å d-spacing with acceptable 10⁻² line broadening. Thus a combination of medium resolution diffraction and SANS is an important aid to the interpretation of small angle scattering data.

(ii) Phase identification.(4)

Larger diameter phases, including those too large to be resolved by small angle scattering, can be resolved at very low volume fractions by high resolution powder diffraction. In practice neutron diffraction allows volume fractions below 1% to be estimated quantitatively. This is appreciably better than is possible with X-rays, where Compton scattering and fluorescence spoil the signal to noise ratio from the minority phase. The techniques of multi-phase Rietveld refinement allow the structure of minority phases to be refined in their normal environment rather than after extraction. Their growth as a function of heat treatment time would be an important application of this instrument. Some phases, such as those from age-hardening alloys, would first appear in SANS, but as their size increased the SANS pattern would become too narrow and the diffraction pattern would become visible by high resolution powder diffraction.

(iii) Internal stress determination.(5)

Neutrons are unique in being able to measure non-destructively the internal stress within a specified volume of a bulk component. The method is the three-dimensional analogue of X-ray surface-stress measurement. High resolution diffraction measures the lattice strain from the small shifts in d-spacing of order 10⁻⁴ in $\Delta d/d$. In order to observe the largest strains the neutron scattering vector Q should be directed along the direction of maximum strain. For many samples this is only possible if the scattering takes place at angles close to 90°. In particular the back-scattering geometry so often used on pulsed sources can often measure the strain only through the Poisson's ratio effect, and so give observed shifts only around a third of the maximum shift. An essential feature of this instrument is therefore the provision of high resolution powder diffraction at 90° scattering angle. The required resolution is of order 3 x 10⁻³ in $\Delta d/d$. A second feature possible with 90° diffraction is the definition of both in-going and out-going neutron beams by apertures to define a scattering volume within a component. Both minority phase analysis and stress analysis can then be mapped out as a function of position within the sample. By rotating the specimen about this position, the full stress tensor can be determined.

(iv) Defect scattering.(6)

For defect sizes below 50 Å electron microscopy becomes increasingly difficult, and often impossible to perform quantitatively. However the Q values between 0.25 to 1 Å⁻¹ needed to observe these sizes are often not accessible using SANS except by changing the counter position or the wavelength. This instrument proposes a special *diffuse scattering* bank with the same relatively relaxed resolution of order $\Delta Q/Q=0.1$ conventional in SANS extending the range of Q values that can be measured simultaneously by SANS. This permits the extension of power-law models revealing the shape of the scattering centres, and giving a good surface area measurement from the Porod law. Perhaps equally important, the extension of the Q range into the region between the first Bragg peak and the origin allows a precise determination of the background. A wide Q range and a precisely subtracted background are the two essentials for successful transformation of SANS results to give the real-space diameter distribution function.

(v) Local ordering.(7)

Disordered systems, such as alloys, glasses, polymers, liquids, gels and ionic solutions, show a diffraction pattern at Q values in the range 0.6 to 3 \AA^{-1} characteristic of local order over distances of a few atomic spacings. Although measurable by X-rays, neutrons enjoy the opportunity of isotopic substitution to give the partial structure factors essential to the understanding of local order. However these are often expensive and available only in small quantities, so that an essential feature of this instrument is its high count-rate and ability to pick out the most appropriate resolution for a particular Q value. This is done by employing a wide range of counter angles. An advantage that neutrons have over X-rays in the area of local atomic ordering is that neutron scattering lengths are constant over the Q range of interest, making possible a cleaner separation of scattering components caused by size effects and by atomic ordering.

(vi) Texture measurement. (8)

Neutron diffraction reveals the preferential alignment of crystallites over an appreciable volume of the sample, and so can give a statistically smooth orientation distribution function (ODF). In contrast X-rays see only a surface layer of crystallites and so give an imprecise ODF depending on the chance number of crystallites within the much smaller beam area. Texture measurements can be made by rotating the sample or, as proposed here, by using many counters spread over a wide azimuthal angle, but with the same scattering angle. Texture variations are then immediately apparent from the azimuthal variation. By using a pulsed beam, several partial pole figures are obtained simultaneously giving inverse pole figures from which the ODF can be obtained from only one, or at most two, sample orientations. The ODF could then be followed as a function of time together with the related microstructural and stress properties. For the interpretation of many mechanical properties in terms of texture, the inverse pole figure along the incident beam direction given by this instrument provides exactly the necessary information.

(vii) Diffusion measurements.(9)

Appreciable diffusion of the molecules in a material leads to a quasi-elastic broadening of the normal elastic scattering. For example the motion of free or bound water molecules can be used to determine the fraction of chemically bound water molecules in a material. The method is complementary to those using nuclear magnetic resonance but can be used in high water content situations where the NMR signal is damped out. The bound molecules will usually give a diffraction spectrum so that simultaneous diffraction would be an important aid in determining the nature of the diffusing species. Quasi-elastic measurements could also give an important guide to the interpretation of SANS from semi-aqueous materials such as setting cement, where the nature of the contrast is not clear. The applications of quasi-elastic scattering extend as the energy resolution is made more stringent. However in practice comparable count-rates between the quasi-elastic scattering and SANS and diffraction are only achieved if a modest energy resolution is specified. The resolution needed to resolve free and bound water is of order 0.1 meV .

(viii) Vibrational spectroscopy.(10)

The vibrational spectrum of materials characterises the strength of the bonds between its molecules. The motions of hydrogen atoms are particularly well seen because of their large cross-section. The vibrational spectra of hydrocarbons reveal their local environment, for example their orientation on a catalytic site. Measurements generally need to be taken over a wide energy range up to a few hundred meV , with a resolution of a few meV . Beryllium filters, including Be/BeO difference techniques, and Be edge differential techniques cover the range adequately with high intensity. The neutron method has two important advantages over infra-red and Raman scattering which cover the same energy range. The neutron scattering intensities are readily calculated on an absolute scale leading to precise interpretation of the results. Secondly the large hydrogen cross-section aids the assignment of modes, which can be identified by deuterium substitution.

The ranges of the scattering vector Q and energy transfer $\hbar\omega$ specified for the multi-facility are summarised in table 2.

3. The design principles of a multi-instrument for the SNS.

It is a unique feature of pulsed neutron scattering that it permits all the neutron techniques described in the previous section to be performed at the same time. This can occur only because the pulsed source is polychromatic and can extend from the cold 4 to 8 Å wavelength neutrons needed for small angle, diffuse and quasi-elastic scattering to the thermal and epithermal 0.1 to 4 Å neutrons needed for diffraction and vibrational scattering. The time-of-flight scans used by all modes of the instrument mean that all the results appear at the same time. A reactor-based instrument with the same objectives would need to scan the incident neutron wavelength over a wide range and so give the results only sequentially.

The Spallation Neutron Source (SNS) at the Rutherford Appleton Laboratory in the UK(11), as the world's highest mean flux fast pulsed source, is the natural site for this instrument. It does impose some important constraints.

- (i) The pulse repetition frequency of the SNS is fixed at 50 Hz. Although this can be reduced by pulse-removal choppers this would not be desirable for many of the modes of this instrument and will not be considered here.
- (i) Its moderators are at ambient, 100K and 20K temperatures. For this instrument with its requirement for good time resolution at thermal energies yet with good cold neutron intensities for small angle scattering the 100K moderator is the best choice.

The key parameter of the multi-facility is its total flight path length L . The period between source pulses $\tau = 20000 \mu\text{s}$ limits the wavelength band $\Delta\lambda$ observable to (12)

$$\Delta\lambda = \frac{hL}{m\tau} = 0.3956 \times \frac{20000}{L(\text{cm})} \text{ \AA} . \quad 1.$$

The required 0 to 8 Å wavelength can be achieved within a single *frame* of the time scan only for a total flight path less than 10 metres. The original design for this instrument had a total flight path of order 20 metres utilising the 0 to 4 Å frame for diffraction and the 4 to 8 Å frame for small angle scattering chosen by a velocity selector *after* the specimen. This had to be rejected because of down scattering through the velocity selector from the intense epithermal flux near the start of the next frame.

Within the key constraint of a total flight path of order 10 metres the remaining parameters must be chosen to satisfy the specifications of table 2, and yet at the same time give appropriate count-rates for key experiments on the various facilities. The arrangement of the counter banks for each facility is shown schematically in figure 1. They were considered with following order of priority:

- (i) The small angle facility.
The resolution requirement $\Delta Q = 0.006 \text{ \AA}^{-1}$ at 8 Å wavelength implies a matched incident and scattered collimation

$$\alpha_0 = \alpha_1 = \frac{\sqrt{2} \lambda \Delta Q}{4\pi} \quad 2.$$

equal to 0.2° . This collimation is sufficiently fine that an incident guide tube is not a sensible option. A nickel guide only achieves 0.2° for wavelengths below 1.2 Å. The natural collimation arising from the moderator width W_m and the incident flight path L_0 is given by

$$\alpha_0^{\text{natural}} = \frac{W_m}{L_0} . \quad 3.$$

With the full SNS moderator width of 10 cm an incident flight path of 27.6 metres is required to give a natural collimation equal to the required value of 0.2° . Thus if the facility is to operate within the required 10 metre total flight path it is essential to employ a converging collimator. These have been successfully used on many SANS facilities (13). The design would employ *pepper pot* irises containing several apertures aligned so that they converge on the detector. The small iris surface means that their

low-angle scattering is reduced. The key parameter is the diameter d_1 of a single aperture at the sample position. This should be matched to the resolution of the counter elements d_2 . We shall assume 0.5 cm for both d_1 and d_2 , as used in many conventional SANS cameras. The scattered flight path L_1 giving the required scattered beam resolution α_1 of 0.2° is given by

$$\frac{\sqrt{d_1^2 + d_2^2}}{L_1} = \alpha_1 \quad 4.$$

or $L_1 = 2$ metres. The constraint that $L_0 + L_1 = 10$ metres then defines the incident flight path $L_0 = 8$ metres. It is assumed that 6 metres of this which passes through the beam shutter and bulk shield of the SNS is available for the converging collimator. The 0.2° constraint then implies an aperture size varying from 0.5 cm diameter at the specimen to 2 cm at the start of the converging collimator and viewing a 2.5 cm diameter area of the moderator. Assuming 8 such apertures distributed over a 10 cm diameter of the moderator surface ensures that half the total moderator area is used. The whole cluster of apertures subtends an angle $\alpha_{cluster} = W_m/L_0 = 0.72^\circ$ and has a diameter of 2 cm at the sample. For experiments performed as a function of position over the sample area using a pencil thin beam, only the central aperture would be used. Very cold neutrons with wavelengths above 8 \AA would be excluded from the beam by reflecting nickel-coated plates.

If the detector active diameter were 32 cm, its maximum angle would be 9.1° , and its Q range for wavelengths above the iron Bragg cut-off of 4.06 \AA would be from 0.004 to 0.24 \AA^{-1} . By using neutrons with thermal energies from 0.5 to 4 \AA the Q range would be extended to cover from 0.01 to 2 \AA^{-1} .

(ii) The back-scattering diffraction facility.

The resolution requirement $\Delta Q/Q = 0.004$ of this facility is chosen to give a high count rate from minority phases. The refinement of new structures is not expected to be a common mode for the facility. With an incident flight path $L_0 = 8$ m and a scattered flight path $L_1 = 2$ m, the overall resolution at a scattering angle ϕ is

$$R = \frac{\delta_m}{L_0 + L_1} + \cot\left(\frac{\phi}{2}\right) \frac{\Delta\phi}{2}. \quad 5.$$

Putting $\delta_m = 2.8$ cm, the back-scattering resolution $R_{180} = 0.003$. For a 2 cm sample and counter element the scattering angle spread $\Delta\phi$ has components of 1.1° from the sample size and 0.72° from the angular spread of the converging collimator giving the specified resolution $R=0.004$ for scattering angles ϕ above 150° . With a maximum scattering angle of 175° , the counter bank extends from a minimum diameter of 8.7 cm to a maximum diameter of 45 cm, to give a total area of order 6000 cm^2 , and subtending a solid angle of 0.6 sterad. The wide d-spacing range extending up to 4 \AA would be particularly valuable for identifying structures in multi-phase problems.

(iii) The 90° stress facility.

The achievement of the specified resolution $\Delta d/d = 0.003$ at scattering angles of 90° is quite demanding. If the timing and angular terms in equation 5 are matched, then the total flight path needs to be of order 13 metres, while the matched angular collimations $\alpha_0 = \alpha_1$ need to be of order 0.2° . Thus high angular collimations are essential and even long guide tube instruments would require additional incident collimation at many wavelengths.

The centre aperture of the converging collimator has the required 0.2° collimation, so that for samples using the 0.5 cm diameter central aperture, the required $\alpha_1 = 0.2^\circ$ collimation could readily be obtained from a single 1.5 cm diameter detector placed 5 metres from the sample. The relatively long scattered flight path increases the total flight path to the required 13 metres, and also gives angular collimation without the use of Soller slits. With the 90° scattering angle a 50 cm long counter subtending 10° in

the vertical plane would not degrade the resolution or the precision of the stress direction to any significant extent. No scattered beam intensity is sacrificed by the long scattered beam flight path. In practice it would need to be inclined at say 30° to the horizontal in order to avoid interaction with neighbouring beam paths.

For larger samples the most important requirement is for sample angles at 45° to the incident beam direction so that the scattering vector Q lies along the length of the specimen. This is particularly true for rod-like test specimens where an external stress needs to be applied parallel to the scattering vector. For this case a focussing technique has been devised to offset the changes in scattering angle across the converging collimator by corresponding changes in the total flight path. The method is detailed in appendix 1. For a counter at a scattering angle ϕ , at a distance L_2 from a thin specimen angled to lie along the scattering vector, focussing occurs when, with the notation of figure 3,

$$(L_0 + L_2) \left(\frac{1}{L_1} - \frac{1}{L_2} \right) = 4 \left(\tan \frac{\phi}{2} \right)^2. \quad 6.$$

For example with $\phi = 90^\circ$, $L_0 = 8$ m and $L_1 = 2$ m the focussing distance when all apertures of the converging collimator arrive with the same flight time is given when $L_2 = 5.12$ m. L_2 decreases as the scattering angle ϕ is reduced, or as the SANS flight path L_1 is reduced. This arrangement allows the full 2cm wide multi-aperture to be used with the resolution appropriate to a single aperture. For most applications a set of 20 counters spaced 0.5° apart and covering scattering angles from 85° to 95° would be acceptable. These counters could be *computer focussed* to give a total scattered beam solid angle of 0.006 sterad with a corresponding increase in effective count rate. The maximum observable d-spacing extends to 4.3 Å, giving a wide range of simultaneously measurable crystal orders.

(iv) The diffuse scattering facility.

The diffuse counter bank is proposed to cover scattering angles from 10° to 30° and so extend continuously the range of Q values covered by the SANS detector. Resolution in $\Delta Q/Q$ can be relaxed back to the 5% level by shortening the flight path to 1 metre. The focussing effect of the converging collimator will be reduced, so we propose a 1cm wide sample and detector element to give an angular spread of 0.8° matching the incident collimation of the whole converging cluster giving around 4% resolution at 30° scattering angle. The Q range for cold neutrons of from 4 to 8 Å will be from 0.15 \AA^{-1} to 0.8 \AA^{-1} . Using thermal neutrons from 1 to 4 Å extends the Q range to 3.2 \AA^{-1} . Although the counter might be used with still shorter wavelength neutrons, its resolution would be insufficient for general amorphous structure determination. It is considered much more important to maintain intensities for the generally weak diffuse scattering by providing full azimuthal detector coverage. This would extend from a radius of 17 cm at 10° scattering to 30 cm at 30° , giving a total area of 6900 cm² and subtending a solid angle of 0.69 sterad.

(v) The local order facility.

The objective of this detector bank is to cover the important Q range from 0.4 \AA^{-1} to 3 \AA^{-1} using a wide variety of wavelengths and resolutions. Both cold and thermal neutron wavelengths are needed. It is proposed to cover the 4 to 8 Å wavelength band using a set of counters from 30° to 150° scattering angles. By employing wavelengths from 1 to 4 Å, the important Q range from 3.2 \AA^{-1} to 12 \AA^{-1} of conventional reactor diffractometers is covered. High resolution diffraction will be performed on other counter banks so that this bank will have a range of more modest Q resolutions of a few percent. With a scattered flight path L_1 of 50 cm, counters 2 cm wide and 20 cm high give 2.3° angular resolution which is sufficient to give $\Delta Q/Q$ of 7.5% at 30° scattering angle, improving to 0.7% at 150° . Spaced every 2.5° in scattering angle, the whole 48 counters would occupy 1900 cm² and subtend 0.77 sterad.

(vi) The texture facility.

For texture measurement to be possible with one or at any rate few sample

orientations, it is necessary to cover as wide a range of scattering angles as possible, both horizontally and vertically. The local order bank provides scattering plane information, but the wide range of wavelengths at which any one reflection is seen makes the immediate interpretation of the texture difficult. It is therefore proposed to build a texture bank on both sides of the sample covering the wide range of azimuthal angles from $+60^\circ$ to -60° at a fixed scattering angle of 100° . The angular spacing between counters need be only 5° to give adequate spatial resolution in the pole figures. 48 counter elements of size $2 \times 4 \text{ cm}^2$ at a 50 cm flight path are proposed. These have a total area of 384 cm^2 and a solid angle of 0.15 sterad. The angular resolution with a 2 cm sample would be 3.2° giving the required resolution $\Delta d/d = 0.03$.

(vii) The quasi-elastic facility.

The LAM spectrometer built by Inoue *et al* in Japan has proved of great utility in materials science (14). The LAM40 instrument uses an incident flight path of 5.7 m and achieves quasi-elastic resolution of 0.1 meV as specified as most useful for the multi-facility. The counter arms are 60 cm to the analyser and 60 cm from analyser to counter. The analyser is a time-focussed array of 100 cm^2 area of pyrolytic graphite of 1.2° mosaic spread. Sample scattering angles of 45° , 60° and 75° are proposed as most suitable for the separation of free and bound water problems.

(viii) The beryllium filter facility.

The required high count rates necessary for including vibrational scattering on a multi-facility are only feasible by using the wide scattered energy window of a beryllium filter. By using a short scattered flight path and large scattered neutron solid angle, energy resolutions of order 10 meV are possible up to around 100 meV energy transfer. The spread in scattered flight times is also minimised by using the shortest possible scattered flight path. A value of 22 cm is proposed. The spread of scattered neutron flight times can also be essentially removed by observing the *beryllium edges* caused by vibrational peaks rather than the peaks themselves. (15)

4. The performance of the multi-facility for key experiments

The essence of a successful multi-facility is that its various components have count rates that enable the required information to be obtained in comparable counting times. It is therefore necessary to consider at this stage a set of key experiments and the information required from them so that the various counter-banks can be appropriately matched. It is by no means a question of equating counter bank solid angles, or even counting rates, since the cross-sections to be measured differ, as does the method of interpreting the data. For example the diameter distribution of an alloy hardening phase needs to be measured in a time comparable to that needed for the volume fraction of an embrittling inter-metallic minority phase, and for measurements of the internal stress and texture in the alloy matrix. The evolution of the glassy structure of cement gel during setting needs to be measured in comparable times to its microporosity distribution, its free to bound water content and its vibrational spectrum. Table 4 lists a set of simple key experiments with well-defined cross-sections for each component of the multi-facility. The counting time for each experiment is calculated using the program SIP (16) for the configuration detailed in table 3 installed on the SNS. The statistical requirements are different for different experiments. For the broad distributions of SANS, defect, local order and vibrational scattering, a requirement of 1% statistical accuracy per resolution element is made. For the stress, texture and quasi-elastic broadening, a requirement of 1% statistical accuracy integrated over the peak is assumed to be sufficient. The SANS, defect, back diffraction, stress and texture experiments are based on an iron or steel sample 2 mm thick. The local order, quasi-elastic, vibrational and SANS calibration are based on a light water sample 1 mm thick. All samples see the same incident flux. For the SNS source with a 1 ev flux of $8 \times 10^{12} \text{ s}^{-1} \text{ ster}^{-1} \text{ eV}^{-1}$ and a Maxwellian total flux of $3.5 \times 10^{12} \text{ s}^{-1} \text{ cm}^{-2}$ the cold neutron flux incident on a full sample is some $4 \times 10^5 \text{ s}^{-1}$ integrated over the wavelength range from 4 to 8 Å. The thermal flux from 0.4 to 4 Å is of order $9 \times 10^7 \text{ s}^{-1}$.

(i) SANS from 0.1% of voids in 2 mm thick steel.

The thermal annealing of irradiated steels suffering from void swelling is a classic example of the need for a multi-facility. The void size distribution broadens, other minority phases are induced – for example ferrite in stainless steel, and distortion stresses are relieved. The SANS contrast from voids is of course unusually large, but it is seen that at 0.05 \AA^{-1} , within the Guinier range $QR_g \approx 2$, the scattering is strong enough to give a 2.3 minute counting time per radial element for 1% statistics.

SANS calibration from 1 mm thick water.

The absolute calibration of SANS intensities is one of its most valuable features. Good 1% statistics per radial element are obtained in a 1.3 hour calibration run.

- (ii) Back diffraction from 1% ferrite in 2 mm thick stainless steel.
The body centred ferrite phase is one of several phases induced by irradiation in stainless steel. At a 1% volume fraction it is typical of the crystalline phases needed to be identified by the back diffraction facility. The 220 peak is considered. At 150° scattering angle it corresponds to $Q = 6.2 \text{ \AA}^{-1}$ at $\lambda = 1.96 \text{ \AA}$. The count rate integrated over the peak is 251 s^{-1} giving 1% statistics in 0.6 mins.
- (iii) 90° stress diffraction from a $3 \times 3 \times 3 \text{ mm}^3$ volume of steel.
For this important application, the integrated intensity of the 220 steel peak is calculated for a pencil beam $3 \times 3 \text{ mm}^2$ in area using just the central aperture of the collimator. The 220 peak is appropriate since its modulus corresponds closely to the isotropic modulus. The counting rate for all 10 counters is 30 s^{-1} giving 1% statistical error in 5.5 mins.

 90° stress diffraction from a 2 mm thick steel plate.
Using the full collimator area in a focussing orientation gives a count rate of 176 s^{-1} integrated over the 220 peak corresponding to 1% statistical error in 0.9 mins.
- (iv) Diffuse scattering from 1% of 25 \AA voids in 2 mm thick steel.
The large range of the pore size distribution potentially measurable using neutrons, if a wide enough Q range can be covered, is most important. The scattering from the smaller end of the void distribution is considered at $Q = 0.5 \text{ \AA}^{-1}$ in the Porod law region ($QR_g \approx 5$). Scattering of 4.4 \AA neutrons then occurs at 20 degrees scattering angle in the diffuse bank. The count rate over a 1 cm annulus is 29 s^{-1} giving 1% statistics in 34 minutes.
- (vi) Texture in 2 mm thick steel.
The integrated intensity of the iron 220 peak is considered measured on a single $2 \times 4 \text{ cm}^2$ element of the azimuthal texture bank at 110° . The count rate is 55 s^{-1} giving 1% statistics in 3 mins. Some 10 pole figures should be measurable simultaneously to give the full orientational distribution function in around 10 mins.
- (vii) Quasi-elastic scattering from a 1mm thick water sample.
Turning again to the 1 mm light water sample, the requirement is to measure the quasi-elastic profile with sufficient statistical precision to enable the area under the broad free water distribution to be separated from the narrow bound water peak. A 1% precision in the integrated area under the whole peak is assumed sufficient for this. The count-rate of a single focussed analyser operating at 4.3 \AA with 0.1 meV resolution is 4.7 s^{-1} giving a 35 minute count time for 1% statistics.
- (viii) Vibrational scattering from 1 mm water at 60 meV energy transfer.
The objective of most neutron vibrational spectroscopy experiments is to identify hydrogenous vibrational modes and so help assign modes and enable inter and intra-molecular force constants to be determined. The vibrations of water molecules are typical and show a broad peak at around 80 meV energy transfer caused by torsional motions. The molecular cross-section at 80 meV is some 35 barns $\text{sterad}^{-1} \text{ eV}^{-1}$. This gives rise to a 20 s^{-1} count rate within a 1 meV scattered energy window. This might be given by a Be/BeO window spectrometer or by a Be edge differential analysis with a 1 meV stepsize. It corresponds to a 8.5 minute run time for 1% statistics.

5. Information presentation: following the *neutron profile* .

A new way of performing neutron experiments is opened up by the multi-facility. The choice of which Q range and resolution is of most importance can be postponed until after the experiment has been completed since the experiment follows the heat treatment or chemical reaction under study, over several ranges and resolutions simultaneously. The battery of facilities would give a *neutron profile* of the sample over any one time period or volume within it. Its display would need great ingenuity to enable the experimenter to follow changes in the profile, rather than be swamped by a deluge of data! It might feature a simultaneous display of processed data. The user would have specified previously the *windows* of interest in which embrittling phase diffraction peaks occur, the unstressed matrix peak positions measured on the 90° counters, and the untextured matrix peak intensities measured on the texture counters. He could then view the changes in the defect size distribution, the embrittling phase volume fraction, the internal stress changes and the texture changes as they occur during the experiment.

6. Conclusions.

The count rate predictions for key experiments given by table 4 show the practicality of this instrument, and its ability to employ all the main techniques of applied neutron scattering simultaneously. Its main advantage is its use in kinetic experiments to relate together the many different processes which may take place at the same time. A second advantage is the neutron economy achieved by the wide range of information gathered in a single experiment. The relatively low cost of a complete process study using this instrument will open the door to project managers at present not able to afford the unique information neutrons can give in materials science.

Appendix 1. Wide angle diffraction focussing using a converging collimator.

The achievement of high resolution in diffraction at wide scattering angles requires a high degree of angular collimation. The following method enables the collimation from a single aperture of a converging collimator to be applied to all its beams. The change in flight time caused by the slightly different scattering angles across the collimator is cancelled by the change in flight path. Figure 3 represents a collimator from the moderator M incident on a sample at distance L_0 and converging on a small angle counter at a further distance L_1 . The sample is placed so as to lie along the bisector to the counter, which is placed at a distance L_2 from the sample at a scattering angle ϕ . The flight time at a displacement x across the sample is given by

$$\begin{aligned} t &= \frac{m(L_0 + L_2)}{h} 2d \sin \frac{\phi}{2} \\ &= \frac{2dm}{h} \left(L_0 + L_2 - 2x \cos \frac{180-\phi}{2} \right) \sin \left(\frac{\phi}{2} + \frac{x \sin \frac{180-\phi}{2}}{2L_1} - \frac{x \sin \frac{180-\phi}{2}}{2L_2} \right) \\ &= \frac{2dm}{h} \left((L_0 + L_2) \sin \frac{\phi}{2} + x \left((L_0 + L_2) \left(\frac{1}{2L_1} - \frac{1}{2L_2} \right) (\cos \frac{\phi}{2})^2 - 2(\sin \frac{\phi}{2})^2 \right) \right). \quad \text{A1.} \end{aligned}$$

Focussing then occurs for any value of x when

$$(L_0 + L_2) \left(\frac{1}{L_1} - \frac{1}{L_2} \right) = 4 \left(\tan \frac{\phi}{2} \right)^2. \quad \text{A2.}$$

For the special case of 90° scattering this reduces to

$$(L_0 + L_2) \left(\frac{1}{L_1} - \frac{1}{L_2} \right) = 4. \quad \text{A3.}$$

References

- (1) *Neutron Scattering Methods of Experimental Physics*, K Skold and D L Price (Eds) Academic Press,(1985).
- (2) C G Windsor, A J Allen, M T Hutchings, C M Sayers, R N Sinclair, P Schofield and C J Wright, *Neutron Scattering in the 90's* IAEA, Vienna (1985) 575.
- (3) G Kostorz, in *Treatise in Materials Science and Technology*, Vol 15, *Neutron Scattering* ,Ed G Kostorz, Academic Press (1979)
- (4) G F Slattery and C G Windsor, *J Nucl Materials* 118 (1983) 165.
- (5) A J Allen, M T Hutchings, C G Windsor and C Andreani, *Adv Phys* (1985) (In Press).
- (6) W Schmatz, in *Treatise in Materials Science and Technology* , Vol 15 in *Neutron Scattering* Ed Kostorz, Academic Press,(1979)
- (7) C N J Wagner, *J of Non Crystalline Solids* 42 (1980) 1.
- (8) H J Bunge, *Technological applications of texture analysis* *Texture of Materials* (Proc 7th Int Con Noordwijkerhowt, (1984) Zwijndrecht 447.
- (9) T Springer, *Quasi-elastic Neutron Scattering for the Investigation of Diffusive Motions in Solids and Liquids*. Springer Tracts in Modern Physics, Vol 64, Berlin,(1978).
- (10) C G Wright and C M Sayers, *Rep Prog Phys* 46 (1983) 773.
- (11) D A Gray in *Neutron Scattering in the 90's* IAEA, Vienna (1985) 261.
- (12) C G Windsor, *Pulsed neutron scattering* Taylor and Francis, London, (1981).
- (13) A C Nunes *Nucl Inst Meth.*, 119 (1974) 291.
- (14) K Inoue, Y Kiyanagi, H Imasa, Y Sakamoto, *Nucl Inst Meth*, 178 (1978) 447.
- (15) J M Carpenter, G H Lander and C G Windsor *Rev Sci Inst* 55 (1984) 1019.

TABLE 1 Neutron scattering compared to other techniques.

	Neutrons	Electrons	X rays	NMR	Light
Microstructure	SANS	TEM	SAXS		
Phases	Diffraction	Diffraction	Diffraction		
Internal strain	90 ⁰ diffraction		Surface diffraction		
Defects	Diffuse	TEM	Diffuse		
Local order	Diffraction		Diffraction		
Texture	Azimuthal diffraction		Diffraction		
Diffusion	Quasi-elastic			Resonance lifetime	
Vibrational	Be filter				Raman Infrared

TABLE 2 Design specification for the multi-facility.

	λ_{\max}	λ_{\min}	Q_{\min}	Q_{\max}	ΔQ_{\min}	$(\frac{\Delta Q}{Q})_{\min}$	$\hbar\omega_{\max}$	$\Delta\hbar\omega$
	Å	Å	Å ⁻¹	Å ⁻¹	Å ⁻¹	percent	meV	meV
SANS	8	4	0.008	0.24	0.004	6		
	4	0.1	0.24	5	0.3	6		
Back diffraction	8	0.1	1.6	125	0.006	0.4		
90° diffraction	8	0.1	1.5	88	0.004	0.3		
Diffuse	8	4	0.15	0.8	0.03	4		
	4	1	0.8	3.2	0.1	4		
Local order	8	4	0.8	3	0.06	0.7		
	4	1	3	12	0.2	0.7		
Texture	4	0.4	2.2	22	0.03	1.5		
Quasi-elastic	4.3	4.3	1	2	0.1	10	5	0.1
Be filter	4	0.1	7.5	21	1	10	200	10

TABLE 3 Proposed parameters of the SNS multi-facility.

Moderator: Liquid methane 100K: 10x10 cm² area: 20000μs period

Incident path: Converging collimator: 8 m flight path: 10 apertures.
Collimation $\alpha_0 = \beta_0 = 0.2^\circ$

Sample 2 x 2 cm² area Standard SNS 40 cm diameter enclosure.

	Scattered path L ₁	Angular range $\phi_{\min} \Delta\phi \phi_{\max}$	Counter elements (widthxheight) xnumber	Total area (cm ²)	Solid angle (sterad)
	(m)	(deg)	(cm ²)	(cm ²)	(sterad)
SANS	2	0(0.14)9	0.5x0.5x12000	3217	0.08
Back diffraction	1	153(1)175	2x2x1526	6107	0.6
90 ⁰ diffraction	5	85(0.5)95	1.5x50x20	1500	0.006
Diffuse	1	10(0.5)30	1x1x6907	6907	0.7
Local order	0.5	30(2.5)150	2x20x48	1920	0.7
Texture	0.5	110	2x4x48	380	0.15
Quasi-elastic:	60 cm sample-analyser: 60 cm analyser-detector: Wavelength 4.3 Å. Graphite analyser: 002 planes: $2\theta_A = 80^\circ$: 10x10 cm ² area: 1 ⁰ mosaic.				
Be filter:	22 cm scattered path: 15 cm thickness: 120–159 ⁰ scattering angle: 10x10 cm ² area: Scattered energy window $\Delta\hbar\omega = 1$ meV.				

TABLE 4 Performance of key experiments on the multi-facility.

	Facility	Experiment	ϕ	Q, ω	Counting Time
			deg.	\AA^{-1} meV	min
(i)	SANS	0.1 % of 100 \AA voids 2mm thick iron.	2	0.05	2.3
		1 mm water calibration.			78
(ii)	Back diffraction	1 % volume fraction 220 bcc peak 2 mm stainless steel.	150	6.2	0.6
(iii)	90 ⁰ stress diffraction	220 bcc peak steel 3x3x3mm ³ volume.	90	6.2	5.5
		2 mm thick plate.			1.0
(iv)	Diffuse	1% of 25 \AA voids 2 mm thick iron.	20	.05	34
(v)	Local order	1% amorphous iron 10 \AA hard spheres 2 mm thick iron.	45	2	16
(vi)	Texture	220 integrated peak 2 mm thick iron.	110	6.2	3
(vii)	Quasi- elastic	1mm thick water Integrated intensity.	45	1.1	35
(viii)	Vibrational	1mm thick water 1 meV window.	140	$\omega=80$	8.5

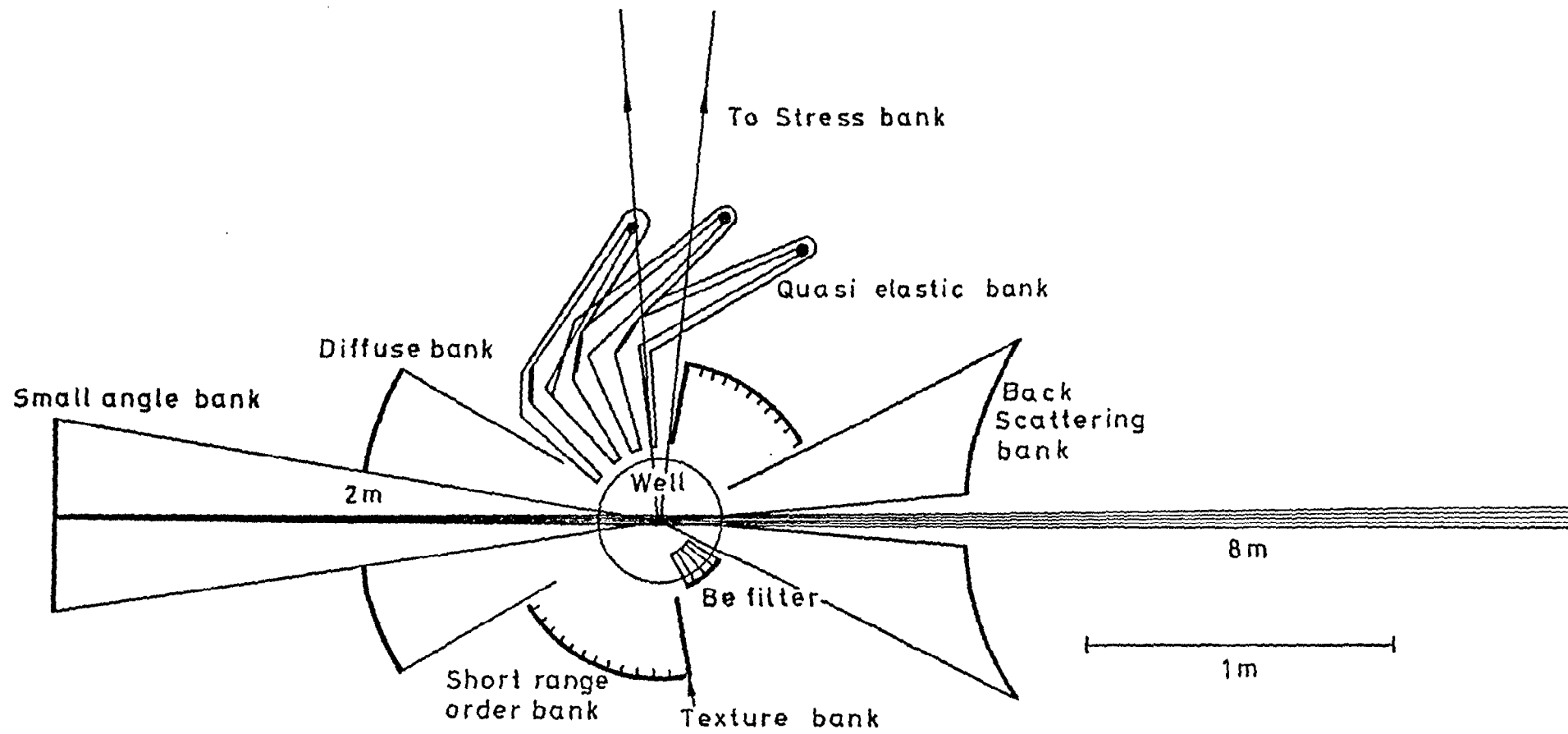


Figure 1. A schematic layout of the proposed materials multi-facility for installation on the SNS. Its various counter banks are able to obtain information simultaneously using the principal techniques of applied neutron scattering.

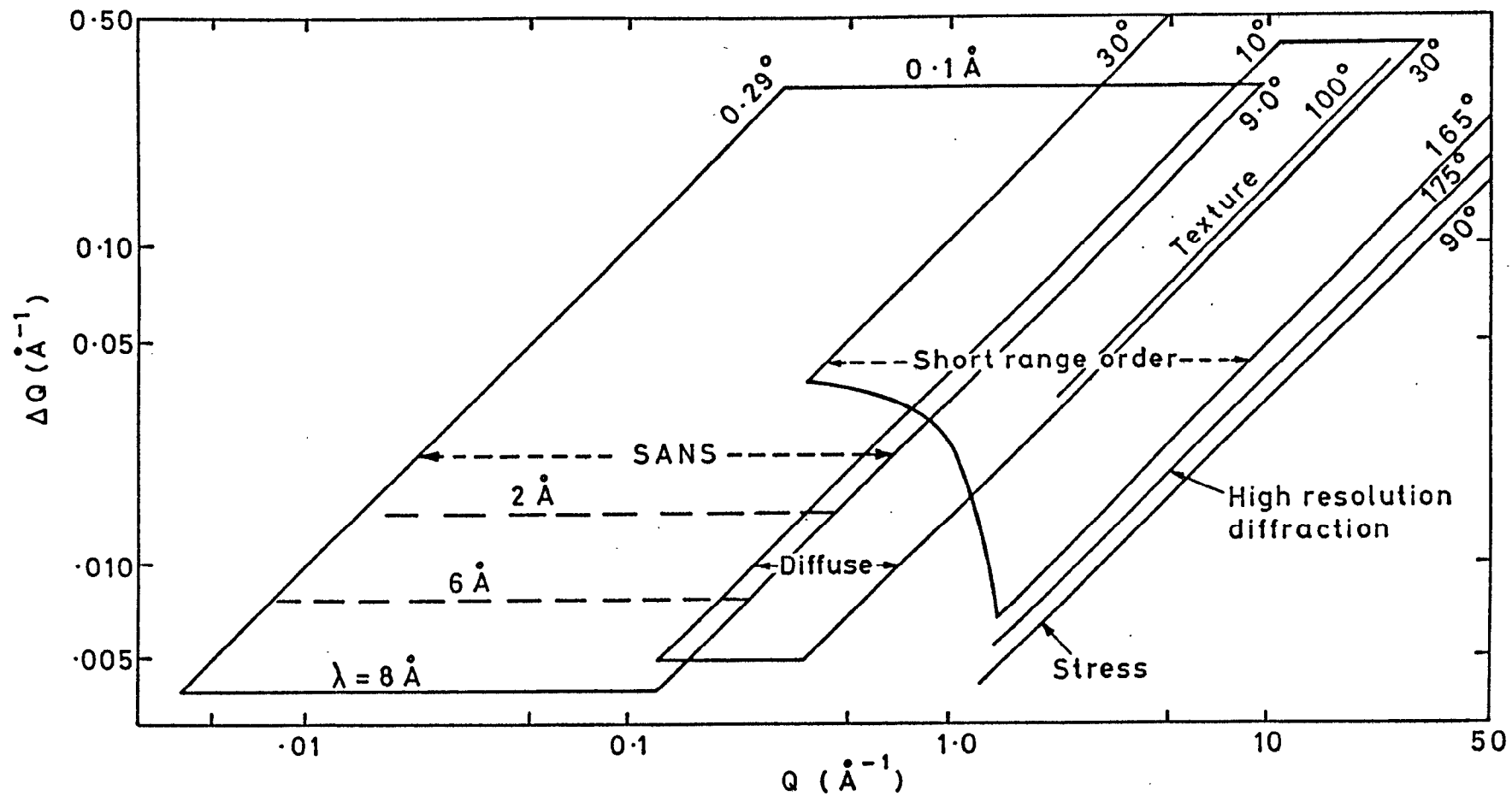


Figure 2. The ranges of scattering vector Q and its resolution ΔQ which can be covered simultaneously using the various counter banks of the multi-facility.

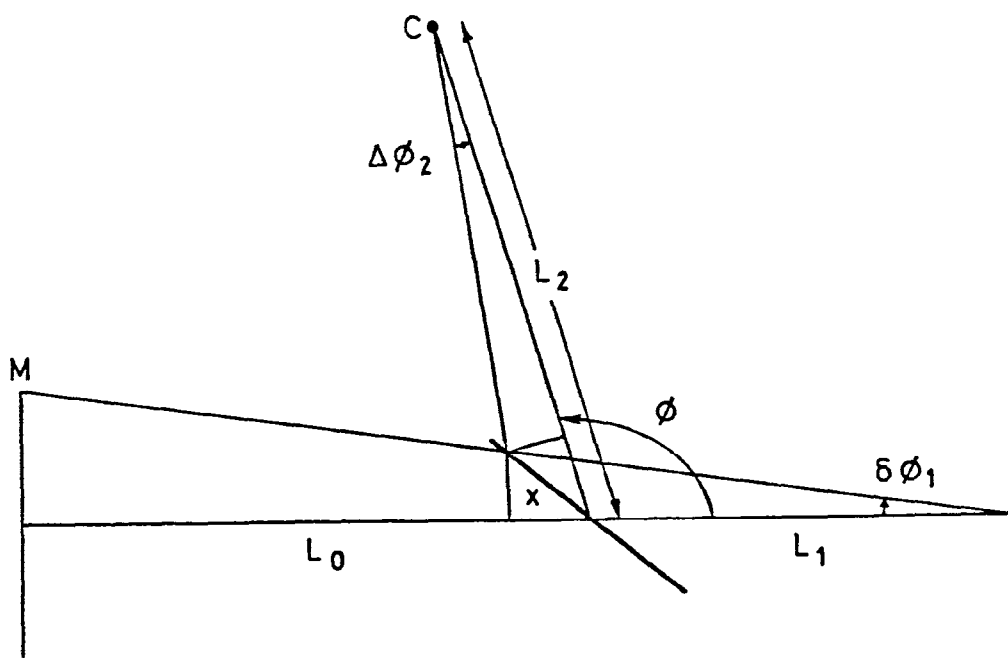


Figure 3. The time focussing for wide angle diffraction possible using a converging collimator.